ConeAct: A Multistable Actuator for Dynamic Materials

Yuyu Lin
yuyulin@andrew.cmu.edu
Human-Computer Interaction Institute, Carnegie Mellon University
Pittsburgh, USA

Jesse T. Gonzalez
jtgonzal@andrew.cmu.edu
Human-Computer Interaction Institute, Carnegie Mellon University
Pittsburgh, USA

Zhitong Cui
zhitongc@andrew.cmu.edu
Human-Computer Interaction Institute, Carnegie Mellon University
Pittsburgh, USA

Yash Rajeev Banka
ybanka@andrew.cmu.edu
Carnegie Mellon University
Pittsburgh, USA

Alexandra Ion
alexandraion@cmu.edu
Human-Computer Interaction Institute, Carnegie Mellon University
Pittsburgh, USA

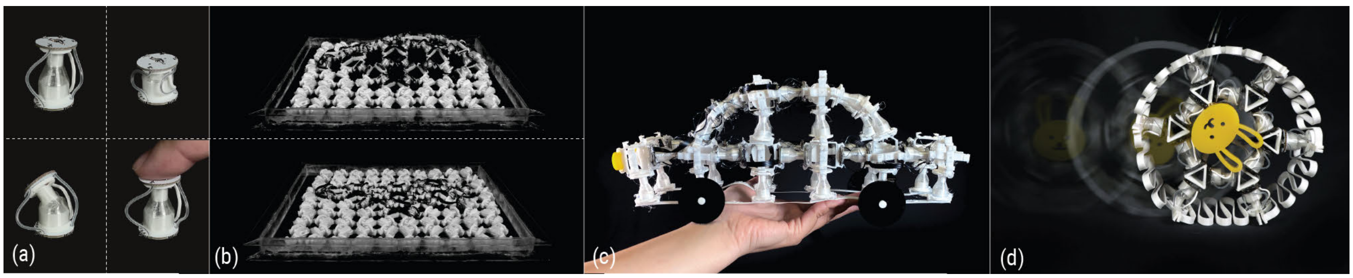

Figure 1: We propose a multistable conical actuator that can compose dynamic materials. (a) This small actuator can switch between multiple states and can take a load passively. We demonstrate the dynamic materials of what we can use this actuator to make, including (b) reconfigurable deployable structures, (c) deformable volumetric prototypes, and (d) self-rolling robots.

ABSTRACT

Complex actuators in a small form factor are essential for dynamic interfaces. In this paper, we propose ConeAct, a cone-shaped actuator that can extend, contract, and bend in multiple directions to support rich expression in dynamic materials. A key benefit of our actuator is that it is self-contained and portable as the whole system. We designed our actuator's structure to be multistable to hold its shape passively, while we control its transition between states using active materials, i.e., shape memory alloys. We present the design space by showcasing our actuator module as part of self-rolling robots, reconfigurable deployable structures, volumetric shape-changing objects and tactile displays. To assist users in designing such structures, we present an interactive editor including simulation to design such interactive capabilities.

CCS CONCEPTS

• **Human-centered computing → Human computer interaction (HCI)**.

CHI '24, May 11–16, 2024, Honolulu, HI, USA

ACM ISBN 979-8-4007-0330-0/24/05.
https://doi.org/10.1145/3613904.3642949

KEYWORDS

Dynamic materials, Fabrication, Programmable Matter

ACM Reference Format:
Yuyu Lin, Jesse T. Gonzalez, Zhitong Cui, Yash Rajeev Banka, and Alexandra Ion. 2024. ConeAct: A Multistable Actuator for Dynamic Materials. In *Proceedings of the CHI Conference on Human Factors in Computing Systems (CHI '24), May 11–16, 2024, Honolulu, HI, USA.* ACM, New York, NY, USA, 16 pages. https://doi.org/10.1145/3613904.3642949

1 INTRODUCTION

Dynamic physical interfaces enable expressive interactions that are difficult to achieve with static structures alone. A dynamic object, for instance, may change shape to better accommodate a user, manipulate other items in its environment, or serve as a platform for haptic feedback. To do so, such objects need to embed actuation, which allows the interface to transition from one form to another.

Today, many of these shape-changing interfaces are composed of smaller, state-changing units. In some cases, these units are electromechanical — rotary motors that form dynamic curves [44], or linear ones that render arbitrary 2.5D shapes [17]. Fluidic, and most often pneumatic actuation [45, 66], is particularly popular for shape-changing interfaces, due to the large force that it can produce while being safe for humans and allow for miniaturized interfaces that can implement wearable tactile feedback [38], can self-assemble into pre-programmed shapes [49], or be integrated into textiles [32].

A key challenge is that actuation is tricky, especially in a desired small form factor. An emerging solution is the use of "active materials" as a method of actuating small shape-changing interfaces [31]. Such materials include shape memory alloys, shape memory polymers, piezoelectric materials, and liquid crystal elastomers—all of which are popular because they can be activated using heat or electricity (i.e., Joule heating) and therefore miniaturize very well. Their utility for simple shape change has been demonstrated in previous work, such as shape-changing thin film interfaces [27, 64], or integrating shape memory alloys into clothing [34, 42].

Though many types of actuators have been developed and used to create dynamic interfaces, an exclusive reliance on "active", power-consuming components means that these interfaces tend not to be portable (i.e tethered to a large compressor, or driven by extensive machinery under-the-hood). By instead leveraging unpowered, multistable structures and combining them with active materials merely as "triggers" that toggle between passive states (with theory support [26]), in this paper, we develop tangible modules that are lightweight, self-contained, and modular to enable users to build and control custom dynamic interfaces.

1.1 ConeAct

ConeAct is a compliant, multistable module that enables the construction of portable dynamic materials. The core component is a hollow, cone-like structure — when this structure is bent, pushed, or pulled, the module snaps into a stable position, holding its state indefinitely without external power (Figure 1a). Critically, this state transition can either by forced externally (i.e. by a human hand) or triggered internally, by active elements integrated within the module. As an actuator, the module can extend, contract, and bend in three directions, to support rich expression in dynamic interfaces.

To achieve this actuation, our module incorporates several shape memory alloy (SMA) wires both inside and outside the passive cone. One coil-shaped wire in the center serves as a "contractor", compressing the module when active; and three straight wires along the perimeter serve as "extenders", allowing the module to stretch and bend. Together, these integrated active and passive elements result in a module that is lightweight and self-contained, enabling the composition of these simple units into more sophisticated, dynamic user interfaces.

1.2 Contributions

We introduce a multistable, actively-toggled module that serves as a "unit cell" for composable shape-changing interfaces. Specifically, we contribute:

(1) A novel combination of a compliant conical structure and a group of SMA wires and coils to make multistable, self-contained, programmable actuators.
(2) An interactive editor for designing dynamic materials composed of our modules and previewing their motions.
(3) Unique compositions of our modules, demonstrating their use as building blocks for shape-changing, interactive applications (deployable data physicalizations, calming tactile displays, deformable design prototypes, and locomoting robots).
(4) A guide to the geometric parameter space of a multistable conical structure, facilitating the design of similar actuators for alternative use cases.

In the remainder of this paper, we demonstrate how this actuator module is an enabling technology for soft, reprogrammable interfaces and materials that can be deformed through computer-controlled actuation as well all by external forces (e.g., manually).

2 RELATED WORK

Our work builds on high-level concepts such as programmable matter and technology such as modular actuators, dynamic materials and multistable structures.

2.1 Dynamic Materials and Programmable Matter

Software is malleable — pixels on a screen can transition from one state to another with ease, enabling an incredible variety of customized interfaces. Meanwhile, in the physical world (of atoms, not bits [29]), researchers have begun working towards parallel goal: a vision of "programmable matter" [20]. Though still nascent, these physical prototypes can change their form and appearance by orchestrating the movement of their constituent components. Such structures have already begun to attract attention for use in scenarios where material reuse is a high priority, such as space exploration [53].

There is a large degree of overlap between "programmable matter" and modular robotics; as in practice, modular robots are how most types of programmable matter are realized today [57]. To allow for large-volume production, many of these robots are designed with simplicity in mind. The thousand robots of the "kilobot" swarm, for instance, are each equipped only with a pair of vibration motors and a few passive bristles for locomotion [56]. Still, this enables them to buzz around flat surfaces and form a diverse array of two-dimensional shapes [59].

At the expense of simplicity (and as consequence, overall module quantity), researchers have also developed modular robots with more sophisticated moving and/or latching mechanisms. These "self-assembling" robots are often either cube-shaped [55] or spherical [36, 60], and can form 3-dimensional shapes by climbing on a scaffold of neighboring modules.

Self-assembly is not the only method of shape-change for these reconfigurable structures. An array of stationary "pin displays" [17] are able to render 2.5-dimensional shapes through the vertical movement of linearly-actuated columns. Others employ rotary motors to enable chain-like structures that bend at the hinges [43]. Our work extends this vision and achieves more complex actuation modes in each unit in a small, portable form factor.

2.2 Modular Actuators as Building Blocks of Dynamic Materials

A common factor among the instances of programmable matter described above is the concept of the "unit cell" — a repeated component that, when combined in large enough quantities, will compose a shape-changing material. Researchers have experimented with a number of different actuators for these unit cells: pneumatic [23, 45, 46], fluidic [32], hydraulic [54], electro-mechanical [25, 44, 65], and magnetic [67]; as well as "active materials" such as shape-memory alloys [34, 42, 61]. These works show the expressiveness of materials composed of modular actuators.

Most of these actuators, however, operate within a single degree of freedom. The machine-knitted pneumatic actuators proposed by Luo et al. [39], for example, can bend, but only in a pre-designated direction. The motor-driven, shape display actuators presented by Hardy et al. [25] allow for displacement, but only along one axis.

In contrast, a few other actuators (our ConeAct module included) can exhibit movement through multiple degrees of freedom. For example, OmniFiber [32] is a thin, fluid-driven actuator that can extend, contract, bend, and coil. MorphIO [45] is a soft pneumatic actuator (containing three air chambers with integrated sensors) that can detect passive manipulation and respond through contraction, extension, and bending. This actuator is conceptually similar to ConeAct, but requires sustained energy to hold its shape. Additionally, as with many pneumatic devices, the associated pumps, valves, and compressors make the system difficult to miniaturize, limiting portability. ConeAct is unique among these actuators – as a relatively self-contained device (requiring only a small battery), it can be used as a *portable* programmable interface.

An SMA is an active material that "remembers" its original shape after deformation, and returns to its original state when heated to a certain temperature. As a resistive element, it can be heated by simply passing an electric current through it, which enables relatively compact designs. In addition, when unpowered, SMAs can be manually reconfigured into arbitrary shapes. These actuators can be miniaturized, and are often integrated into other structures [24, 34, 42, 47, 61]. For example, Patch-O [34] integrates SMA wires or coil into woven patches to achieve bending, expanding, and shrinking for on-skin soft actuation. Springlets [24] also attaches SMA coils into thin and flexible stickers to be worn on various body locations for tactile perception. ClothTiles [42] adds SMA wires into flexible 3D-printed structures that can be attached to clothes. Moon et al. [41] proposes a method that can 3D print shape memory polymers and conductive PLA as an actuator, which can then be sequentially triggered with selective heating. With the slim form factor of the SMA, some researchers developed SMA actuators. For example, Ooide et al. [48] assembled three SMA wires in a silicone tube to create “smart hair” that can bend in three directions. Torres-Jara et al. [63] proposed a unit-cell actuator with SMA sheets activated by Joule heating. Depending on the combination of these unit cells, the designer can control the direction of actuation, the amount of force generated, and the expansion (stroke) of the actuator. However, they require sustained energy to maintain their shape and deform less precisely, especially when bending.

In this work, we use a design approach which leverages the properties of passive, multistable structure in an actuator such that can ensure precise transitions between states and no sustained energy is required to keep its shape. Therefore, this can be promising for the dynamic materials that need to retain their shape for a long time (e.g. a car prototype that should remain static after it has been designed).

2.3 Bistable and Multistable Structures

Multistable structures, and their unique advantages, are readily observable within a number of common objects — collapsible cups and bendable straws, for instance, that maintain their shape after being manually unfolded or collapsed. Each segment of these structures has at least two stable equilibrium states. The transition from one stable equilibrium state to another, or a snap-through action, leads to large deformations [6]. Additionally, these structures can have another stable bent state when they are partially inverted [2]. Researchers have investigated dome-shaped structures, which only have two stable equilibrium states. For example, Brinkmeyer et al. [3] analyzed the effect of different geometric parameters on the response of a type of dome structure to external forces. In our work, we also explored various parameters of our cone-shaped structure, which has a stable bent state, to understand the influence of geometries on actuator design.

In HCI, the bistability property is attractive as the unit for physical logic system [28] and input devices [8], while its potential to combined with active materials is less explored. Kirigami Haptic Swatches [8] involved using the snap-through properties of bistable kirigami structures as a touch input device to enrich the haptic experience for designers. Dementyev et al. [15] provided a bistable display tag using which users can capture and save screenshots from their phones. After the tag is updated, it can continue to present information without further power input. Similarly, Chen et al. [9] proposed a series of bistable modules to maintain the mechanical properties "in memory", which demonstrates the mechanical re-programmability of metamaterials. Even without combining with actuation mechanisms, many works create interesting reconfigurable materials and multistable metamaterials by arranging and coupling passive bistable or multistable geometries [58]. Chen et al. [11] presented a 3D printed bistable structure, and combined them to create tunable pop-up configurations and shape transformations from a planar surface to a 3D shape. Pan et al. [51] fabricated 3D pixel mechanical metamaterials by leveraging an array of segments from commercial flexible drink straws [18, 26]. Our work also utilizes the snap-through mechanism of a bendy straw structures to achieve more degrees of freedom in one unit and more dimensions, e. g., 3D arrangement, of connecting the modules. We also realize the bending stability through the cone shape geometry.

2.4 Active Bistable and Multistable Structures

Among roboticists, the energy-saving advantages of passive, bistable structures have been widely recognized — but to be truly useful in this domain, an active switching element is often incorporated as well [6, 9, 12, 13, 68]. Chi et al. [12] review a number of these implementations. Of particular relevance to our work are instances of soft, bio-inspired structures, with a state-change triggered by heating an embedded SMA element [10, 33]. A more recent example comes from Patel et al. [52], who introduced a bistable membrane, encapsulating SMA coils, that when actuated can serve as a means of robotic locomotion. However, unlike these works, our modules are explicitly designed with *composability* in mind — they are to be assembled into larger, shape-changing structures.

While these active-passive structures are increasingly common in soft robots, they are utilized less often to construct self-actuating materials. Still, some examples (though not always modular) do exist: Gonzalez and Hudson [21] designed an array of electrostatic valves to control the state changing of the bistable dome pneumatically. Overvelde et al. [50] connects balloon-based bistable fluidic soft actuators. Lee et al. [35] connected bistable actuators in chains to make pneumatic snake robots. Faber et al. [16] presented a family of soft sheets with a patterned array of reconfigurable bistable domes that can be actuated pneumatically. Beyond the motion of pop-up and down, in our work, we designed a cone-shaped structure based on the bendable straw mechanism [26] that achieves more degrees of freedom and integrate SMA as active materials to avoid the bulky pneumatic device and achieve portable applications, which benefits rich expression in dynamic interfaces.

3 CONEACT MODULE DESIGN

The mechanism behind our actuator module is based on a conical structure that can hold its shape without external energy, also known as a multistable structure. This allows users to interact with the module manually. In addition, we integrate shape memory polymers to actively control the modules' transition between their stable states. The *key benefits* of this novel design is that it yields a self-contained, small and lightweight, energy-efficient, shape-changing module that can be interacted with passively as well as controlled actively. In this section, we introduce the module's design, properties, interaction, and combination possibilities, before we showcase its applicability in the next section.

3.1 Multistable deformation

Multistable structures can be manipulated into multiple positions and maintain their shape even after users let go. A flexible drinking straw [18, 26] is a popular example of an object that consists of multistable structures. Such straws are made as a single structure with compliant hinges allowing it to fold, stretch, or bend; and the structure can retain its state in each of these configurations. Inspired by the flexible straw, we designed our passive cone structure as a soft truncated cone, sandwiched by two rigid cylinders. Our conical actuator shown in Figure 2 can hold 5 states, i. e., extended, contracted, or bent in 3 positions.

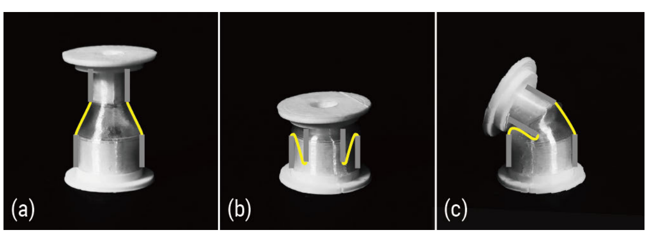

Figure 2: ConeAct has 5 stable states, i. e., an (a) extended state that can snap through to its (b) contracted state, as well as (c) three bent states.

Generally, multistable structures obtain their stable states by embedding flexible struts within rigid walls [2, 69]. The compliant mechanism is designed such that the flexible members are soft enough to deform and pass through the rigid walls holding them. We illustrate this so-called "snap-through" behavior in Figure 3b.

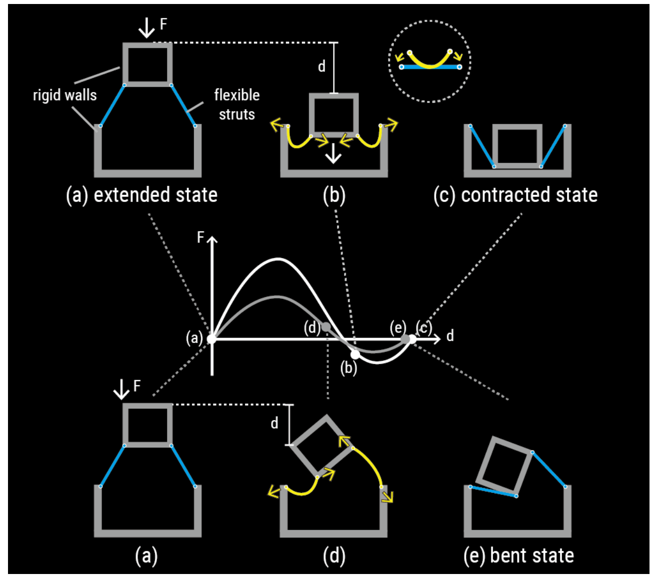

Figure 3: An illustration of the transitions between stable states of our conical structure. ConeAct requires no external force to maintain its shape in the (a) extended, (c) contracted or (e) bent state. When a force is applied on the top of an extended cone, its flexible struts can be curved and have a resisting force against the rigid walls. (b) As the displacement increases, it can snap through to the contracted state. At the snap-through point, the structure starts to pull down, rather than resist the downward force, which is shown in the force(F)-displacement(d) graph as negative force. (d) Similarly, when a force is applied on the side of an extended cone, the flexible struts will bend asymmetrically, and (e) cause the structure to snap to the bent state, where the flexible struts also return to a straight shape but only partially inverted.

After the snap-through, the flexible members can expand in their new position and reach equilibrium. In our conical design, the center section (marked in blue or yellow lines in Figure 3) is flexible enough to deform, while the top and bottom are held in place by rigid cylinders. As Figure 3(d-e) shows, the flexible members can also reach equilibrium when they are partially inverted [2].

3.2 Transitioning between states

To take advantage of our multistable module for building dynamic materials, we add actuation that allows us to control its transition between states. We call our conical actuator module *ConeAct*. To do so, we use active materials due to their small size and potential for miniaturization. In our prototypes, we use shape-memory alloys (SMAs), which are metal alloys that can be deformed by an external force, but return to their "memorized" shape when heated to their transition temperature.

We integrate four such SMAs (here, Flexinol[1]) into our cone structures to push and pull them between their multiple stable states. As shown in Figure 4a, three SMA wires are attached to the

[1]Dynalloy Inc.: https://dynalloy.com

outside of the cone to act as "extenders". These deform passively when the cone collapses, but straighten out when heated to lift the top of the the cone into its extended state. We also integrate a fourth SMA actuator centered within the cone to act as a "contractor", as we show in Figure 4b. This SMA actuator is a coil, which is malleable in its cooled state, but contracts to collapse the cone when heated.

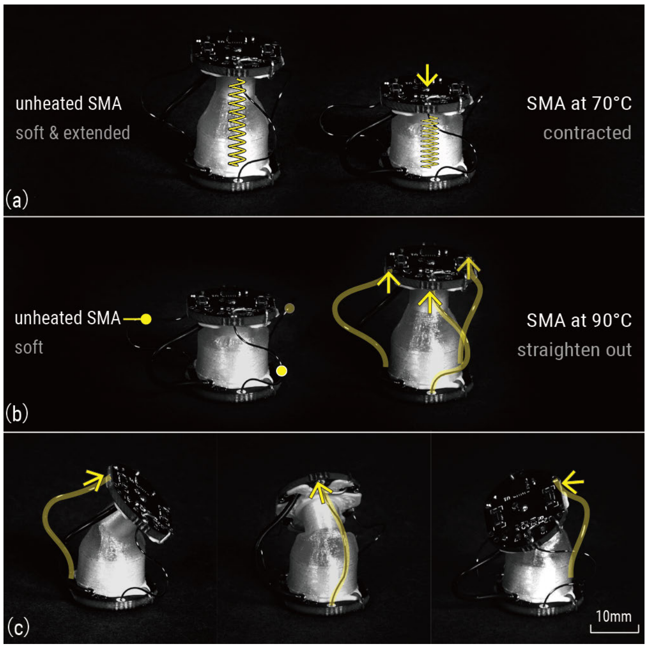

Figure 4: (a) In the extended state, the inner SMA coil is stretched to twice its pre-trained length. When actuated, the coil contracts, and the ConeAct module collapses. (b) In the contracted state, the outer SMA wires ("extenders") are tightly bent. When actuated, these wires straighten out, and the ConeAct module extends. (c) From the contracted state, When one of the outer SMA wires is actuated and straightened out, the ConeAct module bends in the direction opposite to where the wire is located.

The straight SMA wires we use for our prototypes have a transition temperature of 70℃, while the SMA coil transitions at 90℃. We heat our SMAs by running an electrical current through them (i. e., Joule heating). Our prototype implementation of ConeAct can hold its extended state at 25 mm in height, while it is 15 mm tall in its contracted state. The height change (i. e., linear stroke) between these axial stable states, corresponds to 40% of its total height. The three bend states are equally spaced in the azimuthal direction at 0°, 120°, and 240°. We detail the implementation and technical evaluation of ConeAct in Section 4.

With this combination of SMA actuators, we have complete control over the state of our ConeAct module. Note that more than 3 bending states could be achieved, but would require additional SMA actuator to control the states. We decided to limit our prototype to three states to balance assembly complexity and degrees of freedom. Importantly, the electric current is only required for transitioning between the stable states of our engineered cone structure — once actuated, the module will hold its position without drawing any additional power. The combination of the passive multistable structure with this embedded actuation yields our self-contained, small and lightweight, energy-efficient, shape-changing module.

3.3 Sensing user manipulation

Since ConeAct is only actuated to transition between its stable states, but no power is provided to hold the state, it can be manipulated by users safely. As Figure 5 shows, users can manually squeeze or press ConeAct to compress it or bend or stretch the module to assume their desired shape. This becomes especially attractive as multiple ConeAct modules are assembled to assume dynamic interfaces, as we demonstrate with our example applications (Section 6).

To capture the user interaction, we augment ConeAct with sensing capabilities. As we show in Figure 5, ConeAct embeds three simple sensors on its top rim. When users push ConeAct to collapse it, the three sensor pads contact their counterparts that are located on the bottom rim. When ConeAct is bent, only one sensor pair is in contact, which allows us to sense the bending direction. Conversely, when no sensors are contacted, we know that ConeAct is extended. This simple sensing mechanism is intended to detect user interaction. In our experience during development of ConeAct, users tend to push the cone enough to make contact with the contact pads. To detect state changes when the module is self-actuating, thus to enable closed-loop control, an improved sensing structure would need to be developed in the future (e. g., using compliant elastic structures acting as springs on the contact pads to ensure contact is detected).

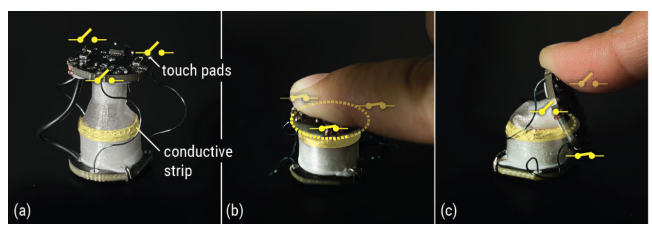

Figure 5: ConeAct can passively detect manipulation by users. (a) ConeAct has three pairs of conductive pads, or three touch switches. We painted the hinge of the conical structures with conductive ink, making it a contact strip. (b-c) When any of the switches touch the contact strip, the conductive pads are connected so that ConeAct can send a signal of the sensed manipulation (pressing or tilting) to the control board.

4 CONEACT IMPLEMENTATION

Designing a multistable structure requires careful choices in both material properties and overall geometry. After an evaluation of multiple parameters (for details, see Section 8) we arrived at the implementation described below.

4.1 Passive Multistable Structure

To achieve multistability in our module, it's important to preserve the rigidity of the upper and lower cylindrical sections, allowing only the conical surface to deform (Figure 2). We accomplish this through the use of a hybrid structure, embedding rigid ABS[2] pieces inside a flexible TPU[3] shell (Shore 85A).

Both the TPU and ABS components are 3D-printed. The walls of the TPU shell are 0.4 mm thick, and the two circular "hinges" (where the snap-through behavior occurs) are slightly thinner, at 0.2 mm. The cylindrical walls of the TPU structure are further rigidized through the insertion of two ABS support rings (0.4 mm thick). This combination maintains the stiffness of the cylindrical sections, and the softness of the conical section. With a negative clearance (-0.1 mm) between the supportive rings and compliant shell, the components are easily, and securely, inserted together.

In its extended state, the cone measures 25 mm. When fully collapsed, the cone is 15 mm tall. In each the three stable bent states, the bend angle is approximately 55° (Figure 6).

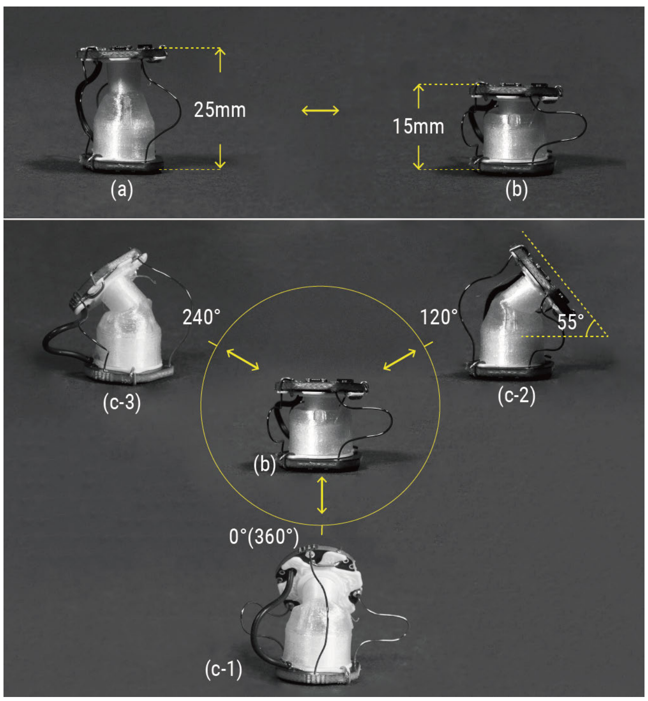

Figure 6: ConeAct has 5 stable states, i. e., an (a) extended state that can snap through to its (b) contracted state, as well as (c-1,2,3) three bent states. The linear stroke between the extended and contracted states of ConeAct is 10 mm, or 40% of the total height. The three bending states actuate at 55°.

4.2 Shape Memory Alloy Actuators

We use a set of four SMA actuators (three straight "extender" wires, and one coiled "contractor" wire) to drive the passive cone from one stable state to another (Figure 4). The extender wires are 0.375 mm in diameter, and approximately 25mm long. When cool (25-30°C lower than transition temperature, which is about 60°C for wires), they can be easily bent, allowing the ConeAct module to rest in a variety of different positions. The contractor coil is made from a slightly thicker wire (0.381 mm), and in its retracted state, collapses to 11 mm. Like the extender wires, it too is malleable when cool (about 40°C), and can be stretched to roughly 22 mm (twice its retracted length).

Figure 7 showcases the assembly process for a single ConeAct module. First, the SMA "extender" wires are cut to 30 mm lengths, and soldered to the bottom PCB, along with the "contractor" coil (Figure 7a). The 3D-printed TPU cone, along with ABS stiffeners, is fixed to the bottom PCB — a small wire is hooked through both the PCB and the ABS stiffener (Figure 7b-c). The cone is then pushed to a retracted, stable state, allowing access to the SMA contractor coil (Figure 7d), which are soldered to the upper PCB (Figure 7e). As a final step, the ABS lid of the cone is glued to the upper PCB (Figure 7f). After the fabrication process, the SMA extenders are approximately 25 mm long (from the lower solder joint to the upper solder joint).

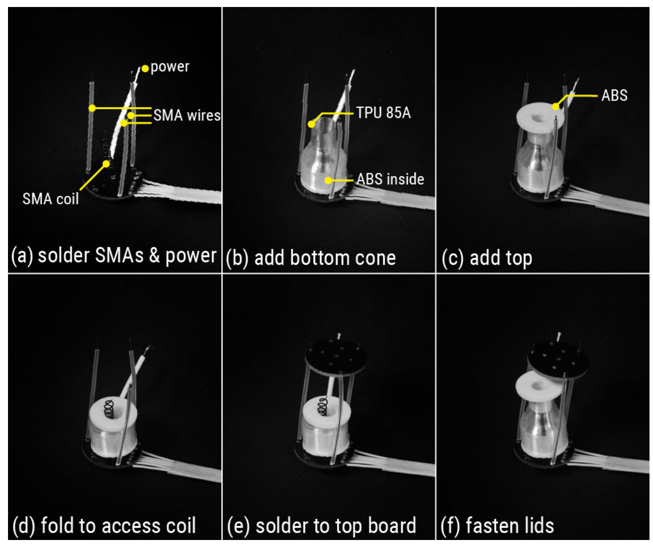

Figure 7: The fabrication process of a ConeAct module. First, (a) SMA wires are soldered to the lower PCB, then (b,c,d) the multistable cone is attached, and finally (e,f) the cone and wires are attached to the upper PCB.

4.3 Electronic Control

Two custom circuit boards (16 mm in diameter) sit on the top and bottom of our ConeAct module (Figure 8). Our SMA actuators are soldered directly to these boards—when we run a current across them, we trigger a shape change, and switch the ConeAct module from one stable state to another.

The bottom circuit board houses two dual MOSFETs[4], each capable of switching up to 5A (though in practice, we limit the current draw to 2.5A). Each MOSFET drain is connected to one end of an SMA wire. The top circuit board acts as a shared power plane, providing a path for the actuator current (a 28 AWG wire connects the two boards, as shown in Figure 8). We drive the gates of the

[2]PolyLite PE01012
[3]Ninjatek 3DNF0817505
[4]Texas Instruments CSD87502Q2

MOSFETs with a small onboard microcontroller (ATTiny1616), operating at 3.3 V. For each actuator, a watchdog timer (which can be set and reset by an external command) will shut off the appropriate MOSFET, to avoid overheating the SMA wire.

The onboard microcontroller responds to commands issued from a separate "director" device (an Arduino Nano) over an I2C bus. (These commands are simple instructions that activate an actuator and set its corresponding timer.) From this director device, we can address and control numerous ConeAct modules (a necessary requirement, since we use multiple modules to compose larger structures).

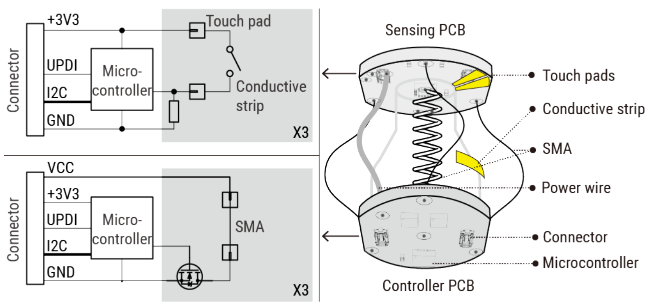

Figure 8: (Left) A simplified schematic of the sensing and actuation circuits. The sensing circuit on the upper circuit board detects electrical contact between conductive regions of the cone structure, when the cone is in a compressed or bent state. (Right) Illustration of the full ConeAct hardware components, with sensing and actuation circuits.

4.3.1 Controlling Multiple Actuators. Our modules can be chained together using flexible connectors that mate with the lower PCB, as shown in Figure 9. Once connected, these modules share a power source and I2C bus, allowing for communication with a single director device. A 3D printed plastic holder, which the modules snap into, can also be used to constrain the actuators in a particular configuration (in Figure 9b for instance, we use a square-shaped holder with flexible hinges). Using these flexible electronic connectors and snap-fit plastic holders, users can assemble and disassemble their modules, therefore reuse them across different applications.

4.3.2 Detecting User Interaction. To sense user interaction with our modules, we add a small amount of conductive material to the top and bottom rims of the cone (Figure 5). The conductive traces on the top rim are connected to pads on the upper printed circuit board, and a circuit is completed when the rims touch. This connection is sensed by three analog inputs on a separate microcontroller (also an ATTiny1616) that resides on the top circuit board. Like the bottom circuit board, this board mates with flexible connectors that join the microcontroller to an I2C bus.

5 INTERACTIVE EDITOR

To assist users in creating their desired dynamic objects, we provide a simple web-based editor. Through this interface, users can design and iterate upon shape-changing structures, by connecting modules together and simulating the resulting motion when actuated.

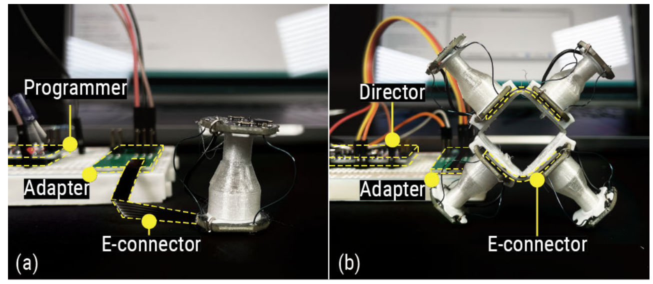

Figure 9: (a) The upper and lower circuit boards are programmed through a UPDI interface, with an Arduino Nano microcontroller acting as a programmer. (b) Multiple modules can be linked together through a combination of flexible electrical connectors and plastic snap-fit holders. They communicate with a director device (a separate Arduino Nano) over an I2C interface.

Figure 10a demonstrates how users may model the base structure of their shape in our editor. In this example, we provide a primitive that combines 4 actuators in a square formation, which can be used to build auxetic structures (such as the application example in Figure 12. Users can also import meshes in our editor, as shown in Figure 10b. This allows them to create more complex models and to work in computer-aided design environments they are already familiar with. Users can import a polygon mesh in popular file formats (*.3dm* or *.stl*). Our editor converts the edges of the imported mesh to ConeAct actuators in their contracted state. The orientation of the placed actuators is aligned with the edge vector, as shown in Figure 10b. The system automatically scales the imported mesh such that only one actuator represents each edge. Our editor expects a model with uniform meshing, i.e., where the edge lengths are approximately the same. Many tools, especially from the graphics community, exist that provide uniform meshing, (e.g., OpenFlipper [40], MeshLab [14], Autodesk Fusion 360 [1]).

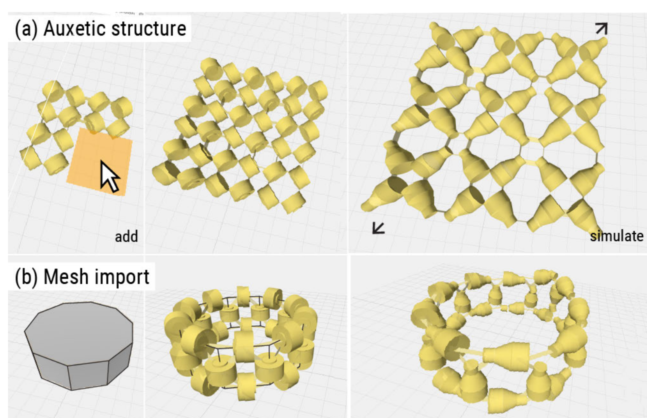

Figure 10: The interface of our editor. Users can (a) create or (b) import meshes and simulate their deformation.

Previewing Motion. Our editor supports users' iterative design by integrating simulation of the actuators' motion. It can simulate the different degrees of freedom of the module while actuated by SMAs, i.e., extended, contracted, and the three bending directions. After verifying their design, users can re-edit the shape or re-select modules for actuation to facilitate design iteration before physical fabrication. Currently, this method can dynamically simulate shape switching, but it does not simulate the deformation of flexible struts on the conical structure. Using the finite element method (FEM) or faster approximation algorithms (such as discrete shells [22]) for more precise simulation presents interesting opportunities for future work.

5.1 Software implementation

Our editor uses *Cannon-es* [4], a lightweight 3D physics engine, to simulate the motion of the multistable actuators, e.g., extension, contraction, and bending. We also use *Three.js* [62] to render the scene and the module's geometry, and use *lil.gui* [37] for the user interface interactions. All the code is written in JavaScript and tested on Google Chrome.

Single Module Simulation. We use *Cannon-es*'s Spring to simulate the different types of motion actuated by SMA wires of the single actuator in the software. We attach three springs to connect the top and bottom sections of the cone geometry, and enable relative movement of these two parts by adjusting the rest length of springs, e.g., setting the rest length of one spring less than the other two for bending motion. When the module is not actuated, the top part and the bottom part of the geometry are joined together with a Cone Twist Constraint [5]. This constraint works by defining a 'cone' of allowable rotational movement, i.e., the aperture angle of the cone, between two rigid bodies, but also remaining a certain distance. Meanwhile, no twist movement is assigned between the two bodies.

Joints between Modules. To approximate the dynamic behavior of multi-actuator materials (i.e. the structures in Figure 10), we apply appropriate joint constraints between the constituent modules. For instance, within the square primitive that composes the auxetic structure (Figure 12), each module is connected by a hinge constraint and a distance constraint, which allows the two simulated actuators to rotate relative to each other while keeping a specific distance. (This corresponds to the flexible physical connector that we use to link modules.) In addition, when the user imports a polygon mesh, the system uses a lock constraint to fix the relative position of each module, which benefits building a steady structure, and the overall shape deformation is only affected by the actuation of modules. In this case, the fabricated connector should be rigid, as in the example we showcased in our rolling robot application (Figure 14).

6 APPLICATIONS

Our ConeAct modules are small, self-contained actuators. A user can assemble them into a desired base-shape, and then dynamically change the shape and properties of the resulting object. As such, our ConeAct module is an implementation of an atomic element of programmable matter [19, 20]. To assemble our modules into dynamic objects, we provide simple mechanical and electronic connectors, as we show in Figure 11.

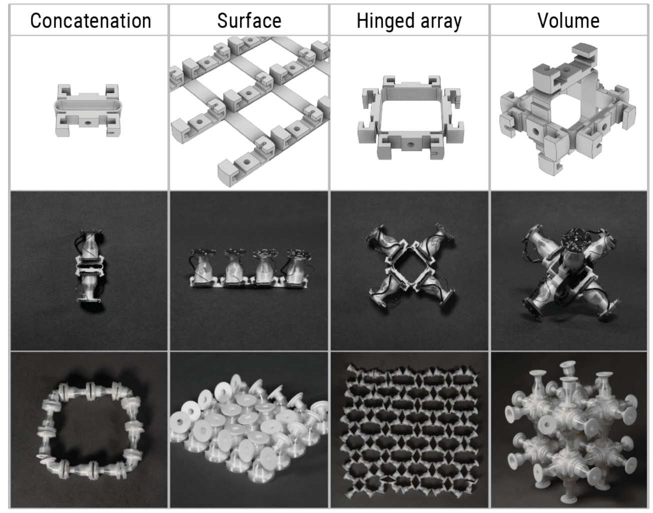

Figure 11: This table shows how modules are connected in series, as a surface, as a hinged array, and as a volume. We designed simple mechanical connectors, which clamp and hold the modules to connect them into different structures, lattices, or objects. These mechanical connectors, in combination with flat electronic wires for communication, allow users to connect our modules to devise different objects.

In the following, we illustrate example applications that demonstrate the utility of such small actuator modules. We showcase how they are useful for remote collaboration serving as dynamic data physicalization displays or for remote product design sessions. We also demonstrate how they can be assembled into a locomotion robot that can bring items to users or into a tactile display that can convey directional information to the user's sense of touch.

6.1 3D Data Physicalization

In the example shown in Figure 12, multiple ConeAct modules assembled in a lattice configuration serve users as a dynamic display for data physicalization. Figure 12a shows how users are exploring and validating data they collected, which their physical ConeAct display in front of them. They pull the display apart to view the data distribution. The display emerges from a flat state into a 3D surface with a smooth distribution. The user understands that their data is normally distributed along the X and Y axes. After performing transformations on the data, users pull the ConeAct display apart again, as shown in Figure 12b. This time, the display expands in both directions, but remains flat. The user realizes that they made an error in their data transformation that accidentally flattened all their data to the plane. Figure 12c shows that after they fix their error, they reveal the correct distribution of their data on the ConeAct display. Our ConeAct display allows users to benefit from the spatial exploration enabled by data physicalization [30].

To achieve this 2D from 3D behavior, we utilize the concept of deployable structures and implement them in a dynamic manner through ConeAct modules. We build on Celli et al. [7], which

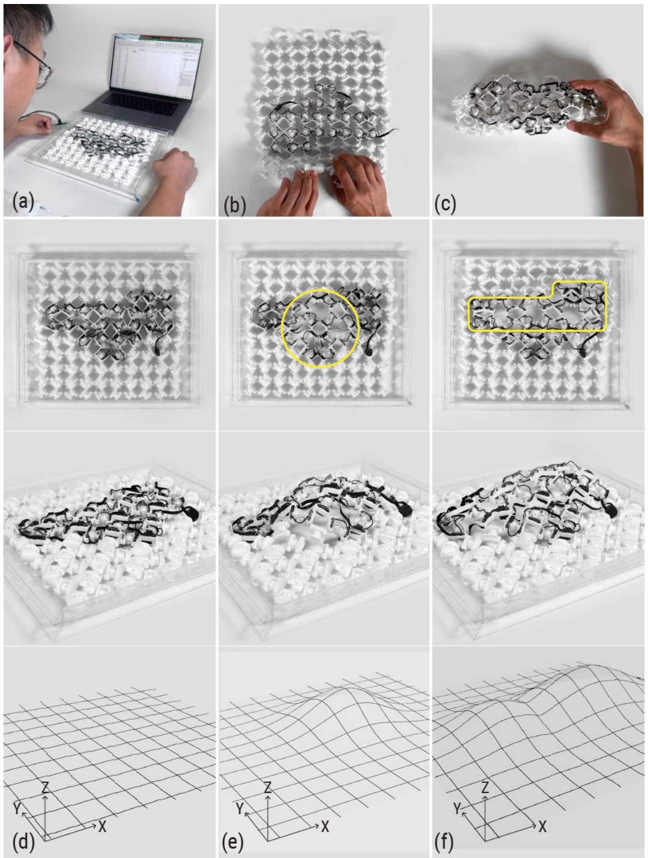

Figure 12: The deployable structure for 3D data physicalization can reconfigure to (e-f) different non-periodic patterns so that will buckle from a flat sheet to a 3D surface. (a) It can help users to inspect and understand the data distribution. (b-c) Users can easily carry a roll of the sheet and carry it with them.

showcased how such deployable structures can be created by passive laser cut sheets. In summary, if its hinged elements have the same length in all dimensions, when manually stretched, the sheet remains flat and extends in all directions, i. e., it behaves like an auxetic material. When some elements are longer, this leads to frustration within the sheet, causing it to buckle out of plane and deploy into a 3D surface. We use this concept, which was shown on passive pre-defined sheets and actuate our ConeAct modules to selectively lengthen or shorten to emerge into a 3D surface. Our modules are assembled using the connectors shown in Figure 11, which implement the basic auxetic behavior.

6.2 Portable dynamic prototypes for design

In Figure 13, we show how ConeAct modules can assist users in collaborative remote product design sessions, even on the go. A product designer is traveling, but has an important deadline coming up. They pack a set of ConeAct modules such that they can participate in remote design meetings during their travel. They connect the ConeAct modules into a volumetric car shape using the connectors shown in Figure 11. As their team members model the center of the car to be shorter, the prototype in the traveler's hands mirrors this change, enabling them to see the remote changes in their physical prototype. The designers iterate over their design collaboratively. Since the ConeAct modules preserve their state passively through their multistable cone geometry and only use power to actuate transitions between states, they can run off batteries making them portable. As Section 7.3 describes, our energy-efficient ConeAct moudles enable users to actuate the design prototypes with a portable phone charger.

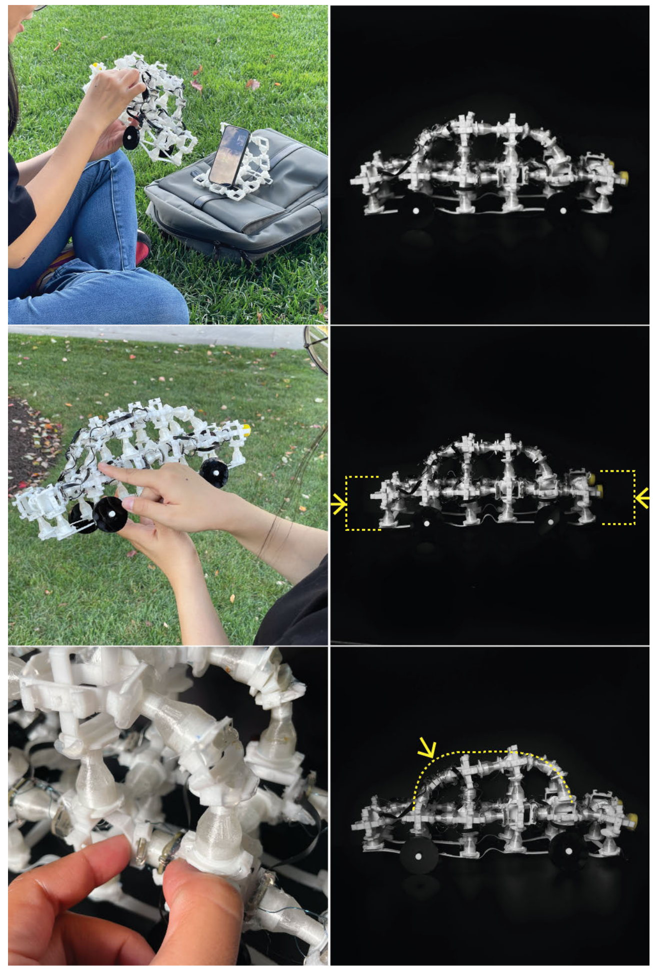

Figure 13: ConeAct modules can be used on the go, due to their low energy requirements. Here, product designers collaborate remotely on a car design. Changes in the car shape are mirrored on the physical prototype.

6.3 Soft rolling robot

ConeAct modules can also be utilized for robotic functions. In Figure 14, we demonstrate a rolling robot that can transport small items to the user. We join 12 ConeAct modules together using rigid triangular connectors, a variation of the connectors shown in Figure 11. Six of these modules serve as extensible "spokes", connected to the interior of a 3D-printed, flexible wheel. (The wheel itself is a compliant, serpentine structure, allowing for the extension and contraction of individual ConeAct modules.)

To trigger its rolling locomotion, we extend the ConeAct module that contacts the floor and its adjacent neighbor module on the inside ring, as illustrated in Figure 14a, which pushes the robot forward. This process utilizes the output force of the multistable property. We repeat this process until the robot reaches its goal position. At the end of its journey, the 6 ConeAct modules on the outer perimeter are bending away from the user to "hand" them the transported object. The robot moves calmly without disrupting the user's attention, yet enters the user's field of view when it's time to deliver the object.

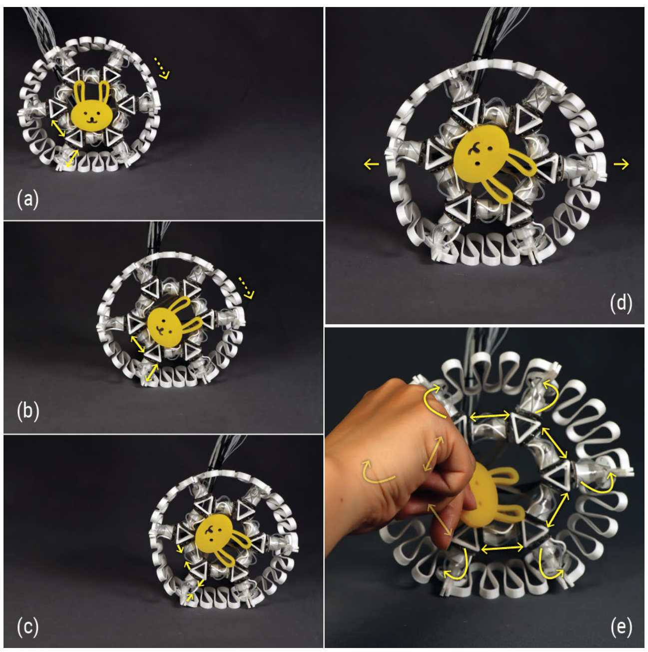

Figure 14: We demonstrate how 12 ConeAct modules are connected to implement a soft rolling robot that can transport small items to users.

6.4 Tactile display

Figure 15 illustrates how ConeAct modules can act as a calming tactile display. In this example application, we connect 15 modules with simple surface connectors, shown in Figure 11b. Additionally, we add 3D printed parts with different textures on the top of each module for variation in tactile textures. The ConeAct modules are actuated in concert, e. g., to hide all spiky tops and only apply gentle directional stroking on the user's palm (Figure 15c). For more intense tactile sensations, the spiky tops are raised, while the round tops are lowered. The tactile sensations paired with the continuous directional strokes and spatio-temporal patterns enable this display to provide a variety of tactile sensations to users.

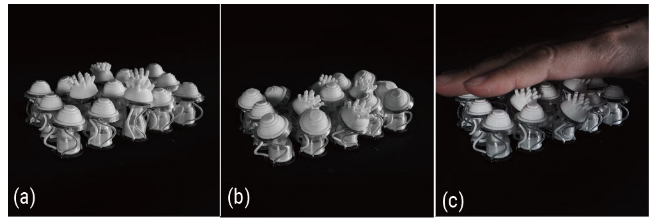

Figure 15: Our tactile display connects 15 modules on a surface. Here, we augment the tops of the modules with textures, which in concert with directional and temporal control can provide calming sensations to users.

7 TECHNICAL EVALUATION

To understand module reliability, and to determine the average time needed to actuate (i.e., contract and extend) a cone, we conducted a series of tests. Since our module is actuated by SMAs, which are thermally activated, we first measured the temperature changes of a ConeAct module in one cycle of its contracting and extending to get an intuition of the relationship between actuation frequency and reliability. Then we conducted three sets of cyclic actuation tests to measure the reliability at three different actuation frequencies, as we describe in the following sections. We note that these tests are intended to enable replicability of our *research prototypes*. As is typical in research, achieving product-readiness will require additional engineering, professional manufacturing, and quality control.

7.1 Thermal Measurement

SMAs are actuated by Joule heating, which triggers them to switch into their programmed form. That means that they need to cool down to become pliable again, such that we can actuate ConeAct's antagonistic SMAs. For example, if ConeAct is actuated into its contracted state, the contractor coil is heated. When we want to extend it again, a heated contractor coil would withstand this antagonistic movement. To better understand appropriate cool down times between actuations, we measured the module's temperature changes during the cooling process after each contraction or extension.

Figure 16 shows our results, captured with a thermal imaging camera (ACEGMET TI256I). Our thermal measurement for *module contraction* (Figure 16 top row) showed that after actuating the coil for 4s, ConeAct switched its state. Within 40s, it cooled down enough to allow us to run cycles repeatedly, although it took 1:34 min (94s) to fully cool down to its original temperature. For *module extension*, we performed the same test, shown in Figure 16 bottom row. Our measurements show that the extender wires switched ConeAct's state within 7s. As opposed to the contractor coil, the extender wires were not enclosed and cooled down within 10s, enabling cyclic actuation. They fully cooled down after 27s in our test.

7.2 Cyclic Actuation Test

We performed cyclic actuation tests between contracting and extending ConeAct. Since the SMAs are heated actively, the main factor influencing ConeAct's performance is their cooling time. To

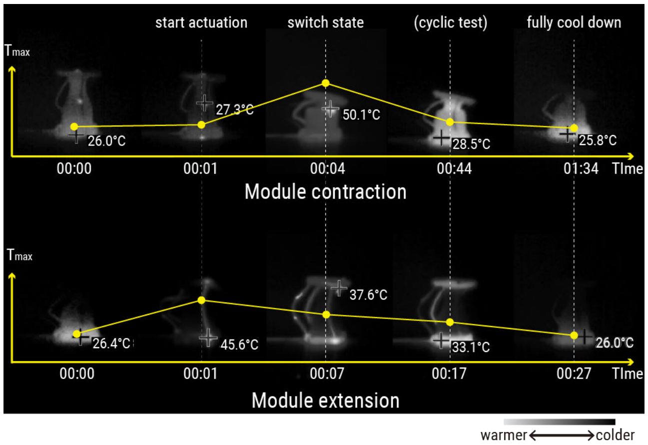

Figure 16: Thermal test results. Changes of the maximum temperature within the field of view during and after module contraction (top) and extension (bottom).

understand this better, we performed a four-step test procedure with *three cooling conditions* (as illustrated in Figure 17):

1. **Slow:** We derived the cooling times from our aforementioned thermal test — letting the SMAs cool passively using 40s for the contractor coil and 10s for the extender wires. We expected ConeAct to actuate reliably between its contracted and extended state.
2. **Fast:** We aimed to test more extreme cases and let the contractor coil cool for only 5s, while keeping extender wires at 10s cooling time. We expected ConeAct to loose reliability, but allow faster transitions.
3. **Active:** We added active cooling to our experiment by placing a miniature cooling fan next to ConeAct. We allowed a cooling time of 15s for the contractor coil and 5s for the extender wires, which we determined empirically. With this shorter test, we expected to verify that ConeAct can increase its reliability using active cooling in the future.

Procedure. We performed our test using the procedure illustrated in Figure 17): (1) We began in the extended state and triggered the transition to the contracted state. We applied current for four seconds through the contractor coil to transition the cone into its contracted state. If it didn't collapse, we kept the current on for two more seconds. At this point, a cone that still remained upright fails the contraction test. (2) The module was then left to cool down according to the cooling conditions described above; i.e., 40s in the *Slow*, 5s in the *Fast*, and 15s in the *Active* cooling condition. (3) To transition from the contracted back to the extended state, we heated each of the extender wires for one second each in a counter-clockwise sequence for up to six seconds in total (i.e., two actuations per extender wire). If at this point a cone remained collapsed, we labeled it as failing the extension test. (4) To conclude one cycle, we left the module to cool down again according to the aforementioned cooling conditions; i.e., 10s for the *Slow* and *Fast*, and 5s for the *Active* cooling condition.

test	contract		extend	
	actuation	cooling	actuation	cooling
Slow	4-6s	40s	6s	10s
Fast		5s		
Active		15s		5s

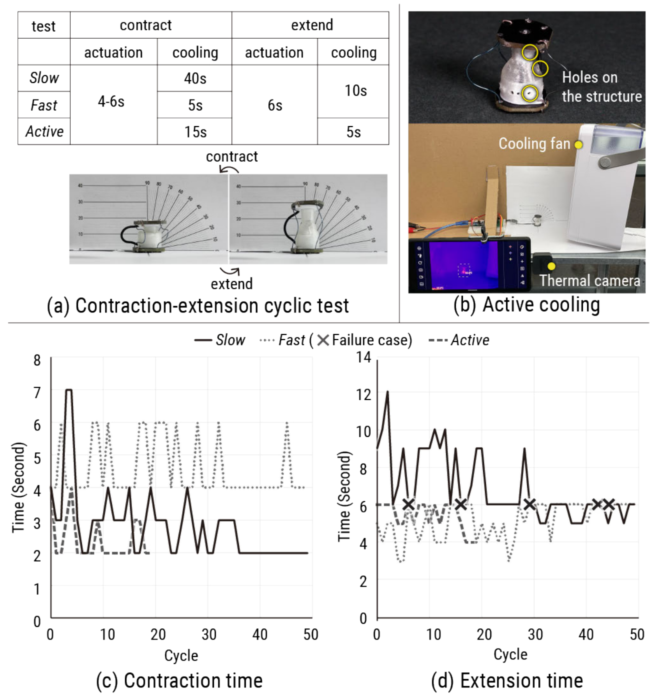

Figure 17: Contraction-extension cyclic test. (a) Test conditions of three repeated contraction-extension actuations of a single ConeAct module. Specifically, three tests have the same actuation duration, but different cooling methods and duration. In *Slow* and *Fast* tests, we let the module cool down at room temperature (26°C during our experiments) in the static air, and in *Active*, we used an active cooling setup shown in (b). (c-d) Results of three cyclic tests. We tested 50 cycles under test conditions 1 and 2 to compare the reliability at different actuation frequencies. The "X" mark on the *Fast* line indicates that the module did not transition to the extended state. We ran 20 cycles for *Active* test to evaluate the effectiveness of the active cooling approach.

The overall time limits (6s for contraction and extension) were chosen to avoid overheating and damaging the module. The initial actuation times (4s for contraction, and 1s per wire for extension) were determined empirically through the evaluation of multiple modules. The SMA wires were driven at 3.5V/2A (average power consumption of 7W when heated). We performed 50 cycles each for the *Slow* and *Fast* cooling conditions, 20 cycles for the *Active* cooling. We video recorded our tests and coded time elapsed to switch the states successfully and failure.

Results. We show our results in Figure 17. We plotted the time it took for the module to expand or contract by calculating the time between the start of the actuation and the module actually switching state based on our video recordings.

In the *Slow* condition, the module successfully switched states for all 50 cycles, without fail. We found that the average contraction time was 2.8s (SD = 1.09s) and the average extension time was 6.86s (SD = 1.73s). Interestingly, both contraction and extension times reduced with increasing number of actuation cycles, yielding a more consistent actuation overall. Specifically, the contraction time remained constant at 2s for the final 14 cycles, and the extension time varied between 5s and 6s for the last 20 cycles. This might be due to the flexible cone being "broken in", i.e., it becoming slightly softer at its hinges, causing it to be deformed more easily by the SMA actuators.

In the *Fast* cooling condition, where we allowed only a 5s cool down phase for the contractor coil, we notice failure cases in extending the module. On five occasions (labeled in Figure 17d), the module failed to extend within the 6s time limit that we pre-determined. Moreover, as cycles increase, it takes longer to extend the cone. Since we don't see failure cases in module contractions, this indicates that the contractor coil has residual heat inside the cone, which is warming the contractor coil and resisting the extender wires. This extreme test confirmed our assumptions that either long passive cooling times or active cooling is necessary.

With the *Active* cooling condition, we verify that active cooling can indeed shorten the actuation cycles to increase interaction speed. Our results confirm that with a 15s cooling time for the contractor coil and 5s for the extender wires, the module switches without fail over our 20 cycles tested. We turned the cooling fan next to the module on only during the cooling phase, not while heating the SMAs. This shorter test confirms that there is room for future work on integrating, e.g., Peltier cooling elements, heat sinks, or similar, to increase the actuation frequency of our modules for programmable matter.

7.3 Energy Consumption

During actuation, each SMA is connected to a 3.5V supply, and draws 2A of current—a power consumption of 7W. Assuming an "on time" of 10s for a full actuation cycle (see previous section), our ConeAct module requires 70J (or 0.02Wh) to contract and extend. To put this in context, using a commonly available portable phone charger[5] (e.g. 10000 mAh at 3.7V, or 37Wh) to power our system, we can expect over 1800 actuations from our system (= 37Wh / 0.02Wh). This level of power consumption, combined with the lightweight nature of our ConeAct modules, makes our system an attractive option for "on-the-go" shape-changing interfaces. As a point of reference, a commonly sold latching solenoid[6] operates at 40W, and while the "on-time" is considerably shorter, the extra weight makes portable applications more challenging.

8 CONE PARAMETER EXPLORATION

In our research prototypes shown in this paper, we aim for small modules that allow us to explore a new modular approach towards programmable matter. However, other researchers might have different goals and use cases and may be interested in larger load-bearing structures. To support others in building on our work, we explore the geometric parameters of our passive multistable cone structure, which is agnostic to the actuation mechanism that triggers the transition between its states, and its resulting mechanical properties.

[5]https://www.amazon.com/Anker-Ultra-Compact-High-Speed-VoltageBoost-Technology

[6]https://www.digikey.com/en/products/detail/delta-electronics/DSML-0630-12P/7427840

8.1 Parameter space

To explore the impact of our cone geometry on its performance, we identified 6 parameters, i. e., size, diameter, wall thickness, hinge height, slope, and strip angle. We illustrate all parameters in Figure 18a. For each parameter, we 3D-printed a range of 4 specimens. Across all experiments, we use the parameters of our ConeAct geometry as a baseline. This yields a total of $6 \times 4 + 1 = 25$ different cone geometries in our experiments. We are mainly interested in understanding how the cone geometry impacts its stability, stiffness, and stroke. We illustrate all results in Figure 19.

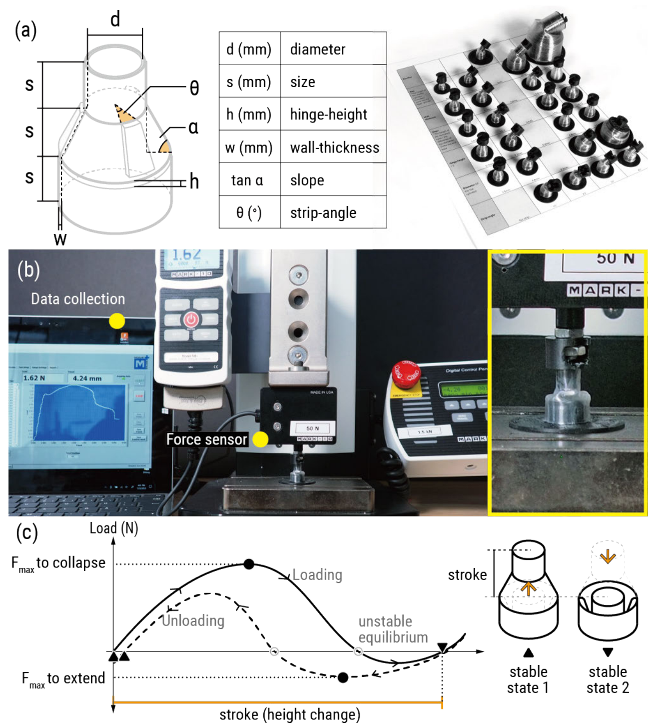

Figure 18: (a) We explore 6 parameters of our passive cone geometry and their influence on the resulting multistability, stiffness, and stroke. The parameters include *s* (size), *d* (diameter), *w* (wall thickness), *h* (hinge height), *α* (slope), and *θ* (strip angle). (b) Test setup for capturing force-displacement data for our multistable cone modules. (c) An idealized force-displacement curve, illustrating bistable behavior.

8.2 Stability tests

Method. We tested the multistability of cone geometries by setting them manually into their contracted or bent position and recording whether they kept that position. Figure 18b shows our simple setup. We recorded 10 minutes of video and registered which cones did not keep their state. We then left the ones that kept their state for this 10 min for about 2 days to confirm that no long-term changes would occur. We depict all cones that kept their states in Figure 19, which the highlighted figures denote long-term stability.

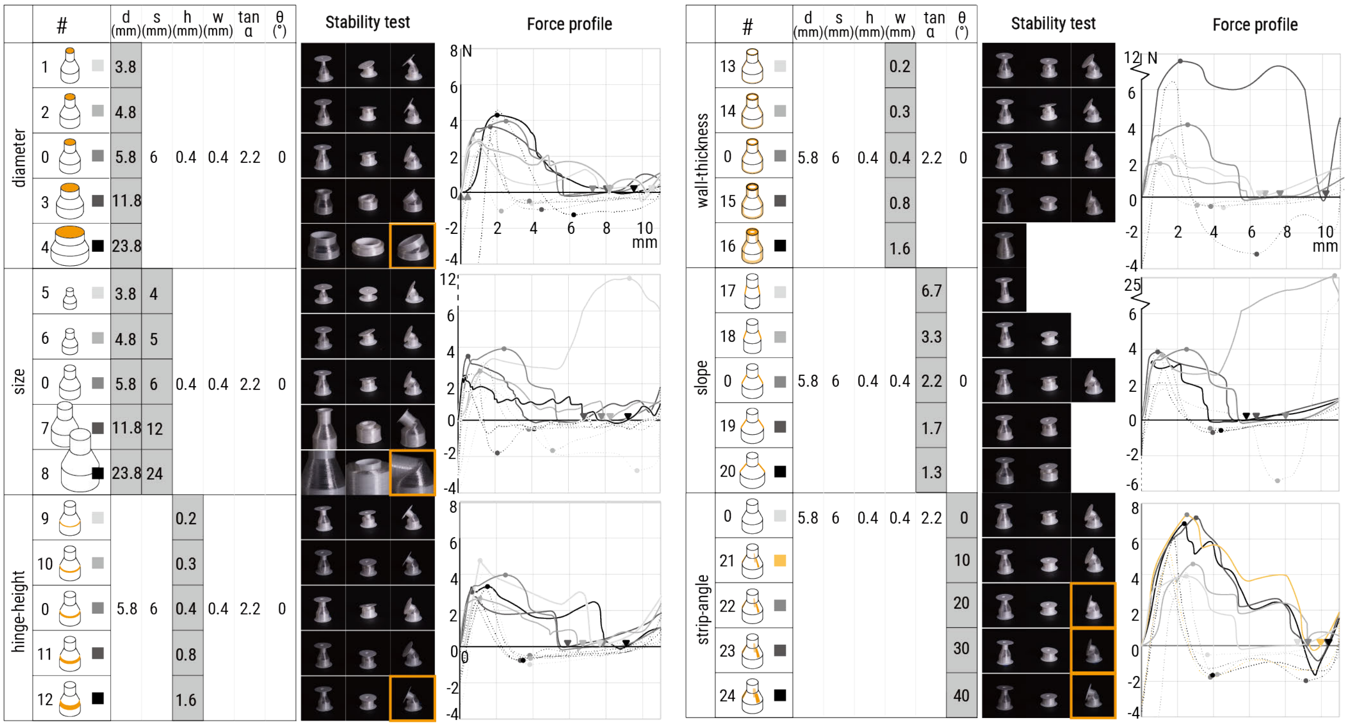

Figure 19: All results of our parameter space exploration. For the results of the stability tests, we present photos of modules that can be bent and highlight modules that can remain bent for more than 2 days. For the force profile, the solid and dashed lines correspond to the contraction and extension processes of the cone, respectively. The dots on each curve indicate the maximum positive or negative force. The triangles on the x-axis indicate when the module switches to steady state 2, with a displacement value corresponding to the stroke. The force profile for the structures we used in our prototypes are highlighted with yellow solid and dashed lines.

Results. Our results for the cones’ *collapsing stability* show that most of them successfully maintain their contracted state. The bistability is only lost when the walls are too thick or when the slope is too small, that is when the cone becomes too cylindrical.

Looking at the cones’ *bending stability*, we found that the slope of the cone influences the bending state stability significantly, with only one slope being stable. Any structures that did not maintain their contracted state also cannot maintain their bent state.

8.3 Force profiles

Method. Beyond the simple stability tests, we also measured how much force it takes to deform our cone structures based on their geometry. We perform compression and tensile tests on our cones using a Mark-10 universal testing machine[7]. We show our setup in Figure 18b, where the top of the cone is fixed to the force sensor using a custom 3D printed lid. The results of these tests are graphs that show how the force changes depending on the displacement.

Results. We give a schematic example of such force-displacement graphs for bistable structures in Figure 18c. We start the tests with the cone in its extended state and perform a compression test. The tester pushed the cone down gradually until it reaches its unstable equilibrium (the first crossing of the x-axis), after which the cone snaps into its contracted state, which is the second crossing of the x-axis. During the snap-through, the cone stops resisting the compression and pulls in the same direction (i. e., down), which shows as negative force. After the cone collapsed, we stopped the compression test and started the tensile test, i. e., we pulled the cone back up. The dashed curve shows the unloading of the cone.

The force-displacement graphs provide insight into the mechanical behavior of the resulting cone and inform of the maximum force needed to collapse or extend the cone. The displacement until the cone reached its contracted state identified the height difference of the cone’s state, i. e., its stroke. These properties can inform designers of the strength needed for their actuators, if they decide to use our cone geometry for different application scenarios and might want to tune their actuators’ e. g., size, stroke length, stiffness for load-bearing scenarios, etc.

The *wall thickness w* influences the stiffness of a cone substantially, as expected. The force-displacement graphs show how the very thin walls at 0.2 and 0.3 mm result in similar stiffness. With growing thickness, the stiffness grows as well. Our tests with 0.4 mm yield a max. force of 4 N, while the 0.8 wall thickness makes the stiffness jump to 11.72 N and the 1.6 mm thick wall exceeds the limit of our 50 N force gauge. Such high stiffness cones can be used

[7] Mark-10 ESM 303 motorized test stand with MR03-10 force sensor (max. 50 N with 0.02 N error)

for load-bearing applications, which in turn require actuators with large enough force to facilitate the transition between states.

The cone *size s* is inversely correlated with stiffness. That is because we isolate the size property from its thickness, i. e., we keep the wall thickness constant for our experiments. This means that cones of the same thickness (i. e., 0.4 mm) have more flexibility, thus making them softer with increasing size. We expect that scaling the cone's thickness proportionally with its size will correlate positively with its thickness.

The *diameter d* of the cone does not seem to have a significant impact on the stiffness or stroke of the cone. However, the increase in diameter increases the cone's volume. This allows engineers to design cones that are large enough hold their desired actuation mechanisms, without impacting the cones' multistability.

The *hinge height h* does not seem to have a significant influence on either the stiffness or the stroke of our cones. Similarly, we don't see the difference in our stability tests—all cones are multistable in compression and bending. Engineers are free to choose a hinge height that fits their fabrication method.

The *slope* α impacts the cone stability significantly with only a narrow range leading to multistable behavior. Steeper slopes result in stiffer cones. However, if the slope becomes too steep, i. e., the cones become increasingly cylindrical, they lose their multistability. The steepest cone (#17) did not compress at all, and while #18 did collapse, it required substantial force. Conversely, more shallow slopes reduce the multistability of the cone geometry as well. The reduction in stability was confirmed by our stability tests, showing that the cones were not stable in their bending positions, by the small area under the 0 N axis in our force-displacement graphs, and by the decreasing stroke, which further indicates weak multistability. In fact our baseline cone with a slope angle of 66° ($= \arctan(\frac{1}{0.45})$) is the only configuration that maintains its stability. We recommend using slopes close to 66° this for such actuators.

The *strip angle* θ influences the cones' stability and stroke length. We call a thickened structure on the flexible walls a "strip". Our baseline cone does not have any strips to avoid confounds with other parameters in our exploration. In this experiment, we see how even narrow strips of 10° double the cones' stroke. With increasing the strip angle, the effect reduces. While the cones' stiffness and stroke increase overall, they remain similar for 20°, 30°, and 40°. We observe that the stability increases with increased strip angle. In our prototypes, we used 10° as the strip angle to remain under the max. force that our SMAs can exert to trigger the state transition.

9 DISCUSSION & CONCLUSION

In this paper, we proposed a novel modular actuator that combines the advantages of multistable structures, which can hold multiple different shapes, and controllable transitioning between the state through active materials (here, shape memory alloys). Our actuator has several *benefits*. It is self-contained and energy-efficient, since it only draws energy during state transitions and can maintain states without consuming power. This self-contained design makes the modules portable and straightforward to combine into various shapes. We showcased four applications to outline ConeAct's utility for calm interactive dynamic interfaces — though we believe that the design space extends beyond this scope as well. In addition to ConeAct's modularity, the combination of passive multistable structures with only brief actuation sequences, enables passive interaction for the user in-situ. Users can simply change the shape of their objects by manually pushing ConeAct modules into different states, without the need for computer control.

However, our research prototypes shown in this paper present some *limitations* as well. SMAs are simple to handle and accessible active materials. Using SMAs enabled us to investigate which applications and interactions such modules can support in the future. The downside is that SMAs are intrinsically slow and our prototypes inherit this property. Additionally, SMAs heat up, which can be solved by adding a heat shield around the modules. In our experiments, we did not incur any injuries due to the comparably short actuation period. Our general design of ConeAct is agnostic to the specific active material used and new active materials that may be discovered in material science can be integrated. For example, 3D printable shape memory polymers with higher power density might enable us to fabricate the passive cone and its active material in one process. This would make the fabrication of the cones less laborious, therefore can enable real-world impact. A simplified fabrication process also promises a substantial miniaturization potential.

On a higher level, we see the main promise of this work in exploring new interactions in the area of programmable matter, i. e., matter that can change its properties upon user input or sensing changes. With our ConeAct modules, that can be assembled to represent and control arbitrary shapes, we contribute to advancing programmable matter and the impact thereof.

ACKNOWLEDGMENTS

We thank Hatice Gokcen Guner for help with setting up the gauge and application prototyping, Dinesh K. Patel and Hugo de Souza Oliveira for their expertise in SMA, Shuhong Wang for skillful photo shooting and editing, and Humphery Yang for valuable suggestions on paper writing. Special thanks to Xiaolei Lu's unwavering support.

REFERENCES

[1] Autodesk. 2023. Fusion 360. https://www.autodesk.com/products/fusion-360/overview Last accessed on April 5, 2023.
[2] Nakul P. Bende, Tian Yu, Nicholas A. Corbin, Marcelo A. Dias, Christian D. Santangelo, James A. Hanna, and Ryan C. Hayward. 2018. Overcurvature induced multistability of linked conical frusta: how a 'bendy straw' holds its shape. *Soft Matter* 14 (2018), 8636–8642. Issue 42. https://doi.org/10.1039/C8SM01355A
[3] A. Brinkmeyer, M. Santer, A. Pirrera, and P.M. Weaver. 2012. Pseudo-bistable self-actuated domes for morphing applications. *International Journal of Solids and Structures* 49, 9 (2012), 1077–1087. https://doi.org/10.1016/j.ijsolstr.2012.01.007
[4] cannon es. 2023. cannon-es. https://pmndrs.github.io/cannon-es/
[5] cannon es. 2023. ConeTwistConstraint. https://pmndrs.github.io/cannon-es/docs/classes/ConeTwistConstraint.html
[6] Yunteng Cao, Masoud Derakhshani, Yuhui Fang, Guoliang Huang, and Changyong Cao. 2021. Bistable structures for advanced functional systems. *Advanced Functional Materials* 31, 45 (2021), 2106231.
[7] Paolo Celli, Connor McMahan, Brian Ramirez, Anton Bauhofer, Christina Naify, Douglas Hofmann, Basile Audoly, and Chiara Daraio. 2018. Shape-morphing architected sheets with non-periodic cut patterns. *Soft matter* 14, 48 (2018), 9744–9749.
[8] Zekun Chang, Tung D. Ta, Koya Narumi, Heeju Kim, Fuminori Okuya, Dongchi Li, Kunihiro Kato, Jie Qi, Yoshinobu Miyamoto, Kazuya Saito, and Yoshihiro Kawahara. 2020. Kirigami Haptic Swatches: Design Methods for Cut-and-Fold Haptic Feedback Mechanisms. In *Proceedings of the 2020 CHI Conference on Human Factors in Computing Systems* (Honolulu, HI, USA) *(CHI '20)*. Association for Computing Machinery, New York, NY, USA, 1–12. https://doi.org/10.1145/3313831.3376655

[9] Tian Chen, Osama R Bilal, Kristina Shea, and Chiara Daraio. 2018. Harnessing bistability for directional propulsion of soft, untethered robots. *Proceedings of the National Academy of Sciences* 115, 22 (2018), 5698–5702.

[10] Tian Chen, Osama R. Bilal, Kristina Shea, and Chiara Daraio. 2018. Harnessing bistability for directional propulsion of soft, untethered robots. *Proceedings of the National Academy of Sciences* 115, 22 (2018), 5698–5702. https://doi.org/10.1073/pnas.1800386115 arXiv:https://www.pnas.org/doi/pdf/10.1073/pnas.1800386115

[11] Tian Chen, Jochen Mueller, and Kristina Shea. 2017. Integrated design and simulation of tunable, multi-state structures fabricated monolithically with multi-material 3D printing. *Scientific reports* 7, 1 (2017), 45671.

[12] Yinding Chi, Yanbin Li, Yao Zhao, Yaoye Hong, Yichao Tang, and Jie Yin. 2022. Bistable and Multistable Actuators for Soft Robots: Structures, Materials, and Functionalities. *Advanced Materials* 34, 19 (2022), 2110384. https://doi.org/10.1002/adma.202110384 arXiv:https://onlinelibrary.wiley.com/doi/pdf/10.1002/adma.202110384

[13] Yinding Chi, Yichao Tang, Haijun Liu, and Jie Yin. 2020. Leveraging monostable and bistable pre-curved bilayer actuators for high-performance multitask soft robots. *Advanced Materials Technologies* 5, 9 (2020), 2000370.

[14] Paolo Cignoni, Marco Callieri, Massimiliano Corsini, Matteo Dellepiane, Fabio Ganovelli, and Guido Ranzuglia. 2008. MeshLab: an Open-Source Mesh Processing Tool. In *Eurographics Italian Chapter Conference*, Vittorio Scarano, Rosario De Chiara, and Ugo Erra (Eds.). The Eurographics Association. https://doi.org/10.2312/LocalChapterEvents/ItalChap/ItalianChapConf2008/129-136

[15] Artem Dementyev, Jeremy Gummeson, Derek Thrasher, Aaron Parks, Deepak Ganesan, Joshua R Smith, and Alanson P Sample. 2013. Wirelessly powered bistable display tags. In *Proceedings of the 2013 ACM international joint conference on Pervasive and ubiquitous computing*. 383–386.

[16] Jakob A Faber, Janav P Udani, Katherine S Riley, André R Studart, and Andres F Arrieta. 2020. Dome-Patterned Metamaterial Sheets. *Advanced Science* 7, 22 (2020), 2001955.

[17] Sean Follmer, Daniel Leithinger, Alex Olwal, Akimitsu Hogge, and Hiroshi Ishii. 2013. InFORM: Dynamic Physical Affordances and Constraints through Shape and Object Actuation. In *Proceedings of the 26th Annual ACM Symposium on User Interface Software and Technology* (St. Andrews, Scotland, United Kingdom) *(UIST '13)*. Association for Computing Machinery, New York, NY, USA, 417–426. https://doi.org/10.1145/2501988.2502032

[18] Joseph Bernard Friedman. 1937. Drinking tube. US Patent 2,094,268.

[19] Seth Copen Goldstein, Jason D. Campbell, and Todd C. Mowry. 2005. Programmable Matter. *IEEE Computer* 38, 6 (June 2005), 99–101. http://www.cs.cmu.edu/~claytronics/papers/goldstein-computer05.pdf

[20] Seth Copen Goldstein and Todd C. Mowry. 2004. Claytronics: A scalable basis for future robots. In *RoboSphere 2004*. Moffett Field, CA. http://www.cs.cmu.edu/~claytronics/papers/goldstein-robosphere04.pdf

[21] Jesse T. Gonzalez and Scott E. Hudson. 2022. Layer by Layer, Patterned Valves Enable Programmable Soft Surfaces. *Proc. ACM Interact. Mob. Wearable Ubiquitous Technol.* 6, 1, Article 12 (mar 2022), 25 pages. https://doi.org/10.1145/3517251

[22] Eitan Grinspun, Anil N. Hirani, Mathieu Desbrun, and Peter Schröder. 2003. Discrete Shells. In *Proceedings of the 2003 ACM SIGGRAPH/Eurographics Symposium on Computer Animation* (San Diego, California) *(SCA '03)*. Eurographics Association, Goslar, DEU, 62–67.

[23] Jianzhe Gu, Yuyu Lin, Qiang Cui, Xiaoqian Li, Jiaji Li, Lingyun Sun, Cheng Yao, Fangtian Ying, Guanyun Wang, and Lining Yao. 2022. PneuMesh: Pneumatic-driven Truss-based Shape Changing System. In *Proceedings of the 2022 CHI Conference on Human Factors in Computing Systems*. Association for Computing Machinery, New York, NY, USA, 1–12.

[24] Nur Al-huda Hamdan, Adrian Wagner, Simon Voelker, Jürgen Steimle, and Jan Borchers. 2019. Springlets: Expressive, Flexible and Silent On-Skin Tactile Interfaces. In *Proceedings of the 2019 CHI Conference on Human Factors in Computing Systems* (Glasgow, Scotland Uk) *(CHI '19)*. Association for Computing Machinery, New York, NY, USA, 1–14. https://doi.org/10.1145/3290605.3300718

[25] John Hardy, Christian Weichel, Faisal Taher, John Vidler, and Jason Alexander. 2015. ShapeClip: Towards Rapid Prototyping with Shape-Changing Displays for Designers. In *Proceedings of the 33rd Annual ACM Conference on Human Factors in Computing Systems* (Seoul, Republic of Korea) *(CHI '15)*. Association for Computing Machinery, New York, NY, USA, 19–28. https://doi.org/10.1145/2702123.2702599

[26] Harry J Harp, Walter T Leible, and William M Mccort. 1968. Flexible drinking tube. US Patent 3,409,224.

[27] Felix Heibeck, Basheer Tome, Clark Della Silva, and Hiroshi Ishii. 2015. UniMorph: Fabricating Thin Film Composites for Shape-Changing Interfaces. In *Proceedings of the 28th Annual ACM Symposium on User Interface Software & Technology* (Charlotte, NC, USA) *(UIST '15)*. Association for Computing Machinery, New York, NY, USA, 233–242. https://doi.org/10.1145/2807442.2807472

[28] Alexandra Ion, Ludwig Wall, Robert Kovacs, and Patrick Baudisch. 2017. Digital Mechanical Metamaterials. In *Proceedings of the 2017 CHI Conference on Human Factors in Computing Systems* (Denver, Colorado, USA) *(CHI '17)*. Association for Computing Machinery, New York, NY, USA, 977–988. https://doi.org/10.1145/3025453.3025624

[29] Hiroshi Ishii, Dávid Lakatos, Leonardo Bonanni, and Jean-Baptiste Labrune. 2012. Radical atoms: beyond tangible bits, toward transformable materials. *interactions* 19, 1 (2012), 38–51.

[30] Yvonne Jansen, Pierre Dragicevic, Petra Isenberg, Jason Alexander, Abhijit Karnik, Johan Kildal, Sriram Subramanian, and Kasper Hornbæk. 2015. Opportunities and Challenges for Data Physicalization. In *Proceedings of the 33rd Annual ACM Conference on Human Factors in Computing Systems* (Seoul, Republic of Korea) *(CHI '15)*. Association for Computing Machinery, New York, NY, USA, 3227–3236. https://doi.org/10.1145/2702123.2702180

[31] C Kaspar, BJ Ravoo, Wilfred G van der Wiel, SV Wegner, and WHP Pernice. 2021. The rise of intelligent matter. *Nature* 594, 7863 (2021), 345–355.

[32] Ozgun Kilic Afsar, Ali Shtarbanov, Hila Mor, Ken Nakagaki, Jack Forman, Karen Modrei, Seung Hee Jeong, Klas Hjort, Kristina Höök, and Hiroshi Ishii. 2021. OmniFiber: Integrated Fluidic Fiber Actuators for Weaving Movement Based Interactions into the 'Fabric of Everyday Life'. In *The 34th Annual ACM Symposium on User Interface Software and Technology* (Virtual Event, USA) *(UIST '21)*. Association for Computing Machinery, New York, NY, USA, 1010–1026. https://doi.org/10.1145/3472749.3474802

[33] Je-Sung Koh, Eunjin Yang, Gwang-Pil Jung, Sun-Pill Jung, Jae Hak Son, Sang-Im Lee, Piotr G. Jablonski, Robert J. Wood, Ho-Young Kim, and Kyu-Jin Cho. 2015. Jumping on water: Surface tension–dominated jumping of water striders and robotic insects. *Science* 349, 6247 (2015), 517–521. https://doi.org/10.1126/science.aab1637 arXiv:https://www.science.org/doi/pdf/10.1126/science.aab1637

[34] Pin-Sung Ku, Kunpeng Huang, and Cindy Hsin-Liu Kao. 2022. Patch-O: Deformable Woven Patches for On-Body Actuation. In *Proceedings of the 2022 CHI Conference on Human Factors in Computing Systems* (New Orleans, LA, USA) *(CHI '22)*. Association for Computing Machinery, New York, NY, USA, Article 615, 12 pages. https://doi.org/10.1145/3491102.3517633

[35] Seonghyeon Lee, Insun Her, Woojun Jung, and Yongha Hwang. 2023. Snakeskin-Inspired 3D Printable Soft Robot Composed of Multi-Modular Vacuum-Powered Actuators. *Actuators* 12, 2 (2023). https://doi.org/10.3390/act12020062

[36] Guanqi Liang, Haobo Luo, Ming Li, Huihuan Qian, and Tin Lun Lam. 2020. Freebot: A freeform modular self-reconfigurable robot with arbitrary connection point-design and implementation. In *2020 IEEE/RSJ International Conference on Intelligent Robots and Systems (IROS)*. IEEE, 6506–6513.

[37] lilgui. 2023. lilgui. https://lil-gui.georgealways.com/

[38] Qiuyu Lu, Jifei Ou, João Wilbert, André Haben, Haipeng Mi, and Hiroshi Ishii. 2019. MilliMorph – Fluid-Driven Thin Film Shape-Change Materials for Interaction Design. In *Proceedings of the 32nd Annual ACM Symposium on User Interface Software and Technology* (New Orleans, LA, USA) *(UIST '19)*. Association for Computing Machinery, New York, NY, USA, 663–672. https://doi.org/10.1145/3332165.3347956

[39] Yiyue Luo, Kui Wu, Andrew Spielberg, Michael Foshey, Daniela Rus, Tomás Palacios, and Wojciech Matusik. 2022. Digital Fabrication of Pneumatic Actuators with Integrated Sensing by Machine Knitting. In *Proceedings of the 2022 CHI Conference on Human Factors in Computing Systems* (<conf-loc>, <city>New Orleans</city>, <state>LA</state>, <country>USA</country>, </conf-loc>) *(CHI '22)*. Association for Computing Machinery, New York, NY, USA, Article 175, 13 pages. https://doi.org/10.1145/3491102.3517577

[40] Jan Möbius and Leif Kobbelt. 2010. OpenFlipper: An Open Source Geometry Processing and Rendering Framework. In *Proceedings of the 7th International Conference on Curves and Surfaces* (Avignon, France). Springer-Verlag, Berlin, Heidelberg, 488–500. https://doi.org/10.1007/978-3-642-27413-8_31

[41] Kongpyung (Justin) Moon, Haeun Lee, Jeeeun Kim, and Andrea Bianchi. 2022. ShrinkCells: Localized and Sequential Shape-Changing Actuation of 3D-Printed Objects via Selective Heating. In *Proceedings of the 35th Annual ACM Symposium on User Interface Software and Technology* (Bend, OR, USA) *(UIST '22)*. Association for Computing Machinery, New York, NY, USA, Article 86, 12 pages. https://doi.org/10.1145/3526113.3545670

[42] Sachith Muthukumarana, Moritz Alexander Messerschmidt, Denys J.C. Matthies, Jürgen Steimle, Philipp M. Scholl, and Suranga Nanayakkara. 2021. ClothTiles: A Prototyping Platform to Fabricate Customized Actuators on Clothing Using 3D Printing and Shape-Memory Alloys. In *Proceedings of the 2021 CHI Conference on Human Factors in Computing Systems* (Yokohama, Japan) *(CHI '21)*. Association for Computing Machinery, New York, NY, USA, Article 510, 12 pages. https://doi.org/10.1145/3411764.3445613

[43] Ken Nakagaki, Artem Dementyev, Sean Follmer, Joseph A Paradiso, and Hiroshi Ishii. 2016. ChainFORM: a linear integrated modular hardware system for shape changing interfaces. In *Proceedings of the 29th Annual Symposium on User Interface Software and Technology*. 87–96.

[44] Ken Nakagaki, Sean Follmer, and Hiroshi Ishii. 2015. LineFORM: Actuated Curve Interfaces for Display, Interaction, and Constraint. In *Proceedings of the 28th Annual ACM Symposium on User Interface Software & Technology* (Charlotte, NC, USA) *(UIST '15)*. Association for Computing Machinery, New York, NY, USA, 333–339. https://doi.org/10.1145/2807442.2807452

[45] Ryosuke Nakayama, Ryo Suzuki, Satoshi Nakamaru, Ryuma Niiyama, Yoshihiro Kawahara, and Yasuaki Kakehi. 2019. MorphIO: Entirely Soft Sensing and Actuation Modules for Programming Shape Changes through Tangible Interaction. In

Proceedings of the 2019 on Designing Interactive Systems Conference (San Diego, CA, USA) *(DIS '19)*. Association for Computing Machinery, New York, NY, USA, 975–986. https://doi.org/10.1145/3322276.3322337
[46] Ryuma Niiyama, Xu Sun, Lining Yao, Hiroshi Ishii, Daniela Rus, and Sangbae Kim. 2015. Sticky actuator: Free-form planar actuators for animated objects. In *Proceedings of the ninth international conference on tangible, embedded, and embodied interaction*. 77–84.
[47] Masaru Ohkubo and Takuya Nojima. 2018. SmartFiber: Reconfigurable Shape Changing Interface. In *Proceedings of the 9th Augmented Human International Conference* (Seoul, Republic of Korea) *(AH '18)*. Association for Computing Machinery, New York, NY, USA, Article 42, 3 pages. https://doi.org/10.1145/3174910.3174949
[48] Yoshiharu Ooide, Hiroki Kawaguchi, and Takuya Nojima. 2013. An Assembly of Soft Actuators for an Organic User Interface. In *Adjunct Proceedings of the 26th Annual ACM Symposium on User Interface Software and Technology* (St. Andrews, Scotland, United Kingdom) *(UIST '13 Adjunct)*. Association for Computing Machinery, New York, NY, USA, 87–88. https://doi.org/10.1145/2508468.2514723
[49] Jifei Ou, Mélina Skouras, Nikolaos Vlavianos, Felix Heibeck, Chin-Yi Cheng, Jannik Peters, and Hiroshi Ishii. 2016. AeroMorph - Heat-Sealing Inflatable Shape-Change Materials for Interaction Design. In *Proceedings of the 29th Annual Symposium on User Interface Software and Technology* (Tokyo, Japan) *(UIST '16)*. Association for Computing Machinery, New York, NY, USA, 121–132. https://doi.org/10.1145/2984511.2984520
[50] Johannes T. B. Overvelde, Tamara Kloek, Jonas J. A. D'haen, and Katia Bertoldi. 2015. Amplifying the response of soft actuators by harnessing snap-through instabilities. *Proceedings of the National Academy of Sciences* 112, 35 (2015), 10863–10868. https://doi.org/10.1073/pnas.1504947112 arXiv:https://www.pnas.org/doi/pdf/10.1073/pnas.1504947112
[51] Fei Pan, Yilun Li, Zhaoyu Li, Jialing Yang, Bin Liu, and Yuli Chen. 2019. 3D pixel mechanical metamaterials. *Advanced Materials* 31, 25 (2019), 1900548.
[52] Dinesh K. Patel, Xiaonan Huang, Yichi Luo, Mrunmayi Mungekar, M. Khalid Jawed, Lining Yao, and Carmel Majidi. 2023. Highly Dynamic Bistable Soft Actuator for Reconfigurable Multimodal Soft Robots. *Advanced Materials Technologies* 8, 2 (2023), 2201259. https://doi.org/10.1002/admt.202201259 arXiv:https://onlinelibrary.wiley.com/doi/pdf/10.1002/admt.202201259
[53] Mark A Post, Xiu-Tian Yan, and Pierre Letier. 2021. Modularity for the future in space robotics: A review. *Acta Astronautica* 189 (2021), 530–547.
[54] Purnendu, Sasha M Novack, Eric Acome, Christoph Keplinger, Mirela Alistar, Mark D Gross, Carson Bruns, and Daniel Leithinger. 2021. Electriflow: Soft Electrohydraulic Building Blocks for Prototyping Shape-Changing Interfaces. In *Designing Interactive Systems Conference 2021* (Virtual Event, USA) *(DIS '21)*. Association for Computing Machinery, New York, NY, USA, 1280–1290. https://doi.org/10.1145/3461778.3462093
[55] John W Romanishin, Kyle Gilpin, and Daniela Rus. 2013. M-blocks: Momentum-driven, magnetic modular robots. In *2013 IEEE/RSJ International Conference on Intelligent Robots and Systems*. IEEE, 4288–4295.
[56] Michael Rubenstein, Alejandro Cornejo, and Radhika Nagpal. 2014. Programmable self-assembly in a thousand-robot swarm. *Science* 345, 6198 (2014), 795–799.
[57] Jungwon Seo, Jamie Paik, and Mark Yim. 2019. Modular reconfigurable robotics. *Annual Review of Control, Robotics, and Autonomous Systems* 2 (2019), 63–88.
[58] Jiahao Shi, Hossein Mofatteh, Armin Mirabolghasemi, Gilles Desharnais, and Abdolhamid Akbarzadeh. 2021. Programmable multistable perforated shellular. *Advanced Materials* 33, 42 (2021), 2102423.
[59] Ivica Slavkov, Daniel Carrillo-Zapata, Noemi Carranza, Xavier Diego, Fredrik Jansson, Jaap Kaandorp, Sabine Hauert, and James Sharpe. 2018. Morphogenesis in robot swarms. *Science Robotics* 3, 25 (2018), eaau9178.
[60] Alexander Spröwitz, Rico Moeckel, Massimo Vespignani, Stéphane Bonardi, and Auke Jan Ijspeert. 2014. Roombots: A hardware perspective on 3D self-reconfiguration and locomotion with a homogeneous modular robot. *Robotics and Autonomous Systems* 62, 7 (2014), 1016–1033.
[61] Yasaman Tahouni, Isabel P. S. Qamar, and Stefanie Mueller. 2020. NURBSforms: A Modular Shape-Changing Interface for Prototyping Curved Surfaces. In *Proceedings of the Fourteenth International Conference on Tangible, Embedded, and Embodied Interaction* (Sydney NSW, Australia) *(TEI '20)*. Association for Computing Machinery, New York, NY, USA, 403–409. https://doi.org/10.1145/3374920.3374927
[62] Three.js. 2023. Three.js. https://threejs.org/
[63] E Torres-Jara, K Gilpin, J Karges, RJ Wood, and D Rus. 2010. Composable flexible small actuators built from thin shape memory alloy sheets. *IEEE Robotics & Automation Magazine* 17, 4 (2010), 78–87.
[64] Guanyun Wang, Tingyu Cheng, Youngwook Do, Humphrey Yang, Ye Tao, Jianzhe Gu, Byoungkwon An, and Lining Yao. 2018. Printed Paper Actuator: A Low-Cost Reversible Actuation and Sensing Method for Shape Changing Interfaces. In *Proceedings of the 2018 CHI Conference on Human Factors in Computing Systems* (Montreal QC, Canada) *(CHI '18)*. Association for Computing Machinery, New York, NY, USA, 1–12. https://doi.org/10.1145/3173574.3174143
[65] Humphrey Yang, Tate Johnson, Ke Zhong, Dinesh Patel, Gina Olson, Carmel Majidi, Mohammad Islam, and Lining Yao. 2022. ReCompFig: Designing Dynamically Reconfigurable Kinematic Devices Using Compliant Mechanisms and Tensioning Cables. In *Proceedings of the 2022 CHI Conference on Human Factors in Computing Systems* (New Orleans, LA, USA) *(CHI '22)*. Association for Computing Machinery, New York, NY, USA, Article 170, 14 pages. https://doi.org/10.1145/3491102.3502065
[66] Lining Yao, Ryuma Niiyama, Jifei Ou, Sean Follmer, Clark Della Silva, and Hiroshi Ishii. 2013. PneUI: Pneumatically Actuated Soft Composite Materials for Shape Changing Interfaces. In *Proceedings of the 26th Annual ACM Symposium on User Interface Software and Technology* (St. Andrews, Scotland, United Kingdom) *(UIST '13)*. Association for Computing Machinery, New York, NY, USA, 13–22. https://doi.org/10.1145/2501988.2502037
[67] Kentaro Yasu. 2022. MagneShape: A Non-Electrical Pin-Based Shape-Changing Display. In *Proceedings of the 35th Annual ACM Symposium on User Interface Software and Technology* (Bend, OR, USA) *(UIST '22)*. Association for Computing Machinery, New York, NY, USA, Article 71, 12 pages. https://doi.org/10.1145/3526113.3545645
[68] Zhenishbek Zhakypov, Kazuaki Mori, Koh Hosoda, and Jamie Paik. 2019. Designing minimal and scalable insect-inspired multi-locomotion millirobots. *Nature* 571, 7765 (2019), 381–386.
[69] Shannon A. Zirbel, Kyler A. Tolman, Brian P. Trease, and Larry L. Howell. 2016. Bistable Mechanisms for Space Applications. *PLOS ONE* 11, 12 (12 2016), 1–18. https://doi.org/10.1371/journal.pone.0168218